SECURITY CLASSIFICATION OF THIS PAGE

AD-A280 979

REPORT DOCUME

DTIC ELECTE JUL 01 1994 S B D

1a. REPORT SECURITY CLASSIFICATION: Unclassified	1b.
2a. SECURITY CLASSIFICATION AUTHORITY	3. DISTRIBUTION / AVAILABILITY OF REPORT: This document has been approved for public release and sale; it's distribution is unlimited
2b. DECLASSIFICATION / DOWNGRADING SCHEDULE	
4. PERFORMING ORGANIZATION REPORT NUMBER(S): Technical Report #4	5. MONITORING ORGANIZATION REPORT NUMBER(S): 4133046
6a. NAME OF PERFORMING ORGANIZATION: University of Minnesota; 6b. OFFICE SYMBOL (If applicable): ONR	7a. NAME OF MONITORING ORGANIZATION: Office of Naval Research
6c. ADDRESS (City, State, and ZIP Code): Dept. of Chemical Eng. & Materials Science, University of Minnesota, Minneapolis, MN 55455	7b. ADDRESS (City, State, and ZIP Code): 800 Quincy Street North, Arlington, VA 22217-5000
8a. NAME OF FUNDING / SPONSORING ORGANIZATION: Office of Naval Research; 8b. OFFICE SYMBOL (If applicable): ONR	9. PROCUREMENT INSTRUMENT IDENTIFICATION NUMBER: Grant NO0014-93-1-0563
8c. ADDRESS (City, State, and ZIP Code): 800 North Quincy Street, Arlington, VA 22217-5000	10. SOURCE OF FUNDING NUMBERS: PROGRAM ELEMENT NO. / PROJECT NO. / TASK NO. / WORK UNIT ACCESSION NO

11. TITLE (Include Security Classification)

Nanoscale Imaging of Molecular Adsorption

12. PERSONAL AUTHOR(S)

H. Cai, A. C. Hillier, K. R. Franklin, C. G. Nunn and M. D. Ward

13a. TYPE OF REPORT	13b. TIME COVERED	14. DATE OF REPORT (Year, Month, Day)	15. PAGE COUNT
Technical	FROM 5/1/93 TO 6/30/94	6/23/94	17

16. SUPPLEMENTARY NOTATION

17. COSATI CODES: FIELD	GROUP	SUB-GROUP	18. SUBJECT TERMS (Continue on reverse if necessary and identify by block number)
			Organic Conductors/Atomic Force Microscopy/Nucleation/ Fractals

19. ABSTRACT (Continue on reverse if necessary and identify by block number)

The adsorption of organic molecular species onto highly ordered, chemically well defined substrates may provide insights into the intermolecular interactions, molecular recognition, and aggregation phenomena responsible for the formation of organic thin film and solid state assemblies. The advent of scanning probe microscopy, particularly the atomic force microscope, now provides a method for observation of these adsorption processes on the molecular level. We herein report atomic force microscope observations of the adsorption of anions of the organic di-acid 5-benzoyl-4-hydroxy-2-methoxybenzenesulfonic acid from aqueous solution onto the (0001) surface of hydrotalcite, a layered anionic clay. This adsorption process is believed to mimic the ion exchange reactions that commonly occur within the layers of hydrotalcite. Atomic force microscope images reveal that the coverage of the adsorbed anions depends upon the total charge of the anion (1- or 2-). This is due to electroneutrality requirements associated with coulombic interactions between the cationic hydrotalcite surface and the anionic molecules. The AFM data, along with consideration of coulombic interactions and hydrogen bonding between three-fold clay hydroxyl sites and the sulfonate moiety on the anions, enables tentative assignment of the orientation of the anions with respect to the hydrotalcite surface

20. DISTRIBUTION / AVAILABILITY OF ABSTRACT	21. ABSTRACT SECURITY CLASSIFICATION
☒ UNCLASSIFIED/UNLIMITED ☐ SAME AS RPT ☐ DTIC USERS	Unclassified
22a. NAME OF RESPONSIBLE INDIVIDUAL: Robert Nowak	22b. TELEPHONE (Include Area Code): 703-696-4409 / 22c. OFFICE SYMBOL: ONR Code 1113

DD FORM 1473, 84 MAR — 83 APR edition may be used until exhausted. All other editions are obsolete

SECURITY CLASSIFICATION OF THIS PAGE

Unclassified

OFFICE OF NAVAL RESEARCH

GRANT # N00014-93-1-0563

R&T Code 4133046

Technical Report # 4

"Nanoscale Imaging of Molecular Adsorption"

by

H. Cai, A. C. Hillier, K. R. Franklin, C. G. Nunn and M. D. Ward

Prepared for Publication

in

Science

Department of Chemical Engineering and Materials Science
University of Minnesota
Amundson Hall
421 Washington Ave. SE
Minneapolis, MN 55455

June 20, 1994

Nanoscale Imaging of Molecular Adsorption

Heng Cai[†], Andrew C. Hillier[¥],
Kevin R. Franklin[††], C. Craig Nunn[†], and Michael D. Ward[¥,*]

[†]*Unilever Research U.S. - Edgewater Laboratory*
45 River Road, Edgewater, NJ 07020

[¥]*Department of Chemical Engineering and Materials Science , University of Minnesota,*
Amundson Hall, 421 Washington Ave. SE, Minneapolis, MN 55455

[††]*Unilever Research U.S.-Part Sunlight Laboratory,*
Quarry Road East, Bebington, Wirral L63 3JW, U.K.

The adsorption of organic molecular species onto highly ordered, chemically well defined substrates may provide insights into the intermolecular interactions, molecular recognition, and aggregation phenomena[1] responsible for the formation of organic thin film and solid state assemblies.[2] The advent of scanning probe microscopy, particularly the atomic force microscope,[3] now provides a method for observation of these adsorption processes on the molecular level.[4] We herein report atomic force microscope observations of the adsorption of anions of the organic di-acid 5-benzoyl-4-hydroxy-2-methoxybenzenesulfonic acid[5] from aqueous solution onto the (0001) surface of hydrotalcite, a layered anionic clay. This adsorption process is believed to mimic the ion exchange reactions that commonly occur within the layers of hydrotalcite. Atomic force microscope images reveal that the coverage of the adsorbed anions depends upon the total charge of the anion (1- or 2-). This is due to electroneutrality requirements associated with coulombic interactions between the cationic hydrotalcite surface and the anionic molecules. The AFM data, along with consideration of coulombic interactions and hydrogen bonding between three-fold clay hydroxyl sites and the sulfonate moiety on the anions, enables tentative assignment of the orientation of the anions with respect to the hydrotalcite surface.

*Author to whom correspondence should be addressed
Version 1.10: 3/29/93
To be submitted to *Nature*:

Layered clays are of scientific and potential technological interest due to their utility as ion exchange materials,[6] catalysts,[7] antacids,[8] catalytic supports,[9] and modified electrodes.[10] The recent observation that clays preferentially adsorb one enantiomer when exposed to mixtures of L- and D-histidine has led to the suggestion that the stereoselective adsorption-desorption of molecules on clays may be related to the origin of chirality in living systems.[11] Hydrotalcite, $Mg_6Al_2(OH)_{16}CO_3 \cdot 4H_2O$ (HT), which crystallizes as hexagonal plates in the rhombohedral $R\bar{3}m$ space group is representative of anionic clays (Figure 1).[12] These crystals consist of alternating cationic $Mg_6Al_2(OH)_{16}^{2+}$ and anionic $CO_3^{2-} \cdot 4H_2O$ layers (Figure 1b). The cationic layers comprise metal hydroxide octahedra, which share edges to form densely packed, positively charged, brucite-like sheets terminated by hydroxyl groups and exhibiting hexagonal symmetry. The stoichiometry of HT dictates an overall 2+ charge per $Mg_6Al_2(OH)_{16}$ unit. The charge on these metal hydroxide sheets is compensated by the anions in the interstitial layers, which can be exchanged with other anions such as Cl^-, NO_3^-, and SO_4^{2-} under appropriate conditions.[13,14]

The hydroxyl and metal atom positions within the HT (0001) layers exhibit a hexagonal motif with metal-metal and hydroxyl-hydroxyl spacings of 3.1 Å. However, ordering of the metal-hydroxide sheets with respect to the metal atoms has not been clearly established, although some reports have suggested supercells that implicate ordering of the Mg and Al atom positions.[15] The interstitial anion layers are always disordered in these clays.[16] This presence of two different metal atoms in the metal-hydroxide layer renders the accompanying hydroxyl sites inequivalent. Notably, a $Mg_6Al_2(OH)_{16}^{2+}$ layer that exhibits order with respect to the metal atom positions will have 25% of the hydroxyl groups bonded to three Mg atoms (Mg_3 sites), with the remaining 75% bonded to two Mg and one Al (Mg_2Al sites) (Figure 1c). The Mg_3 hydroxyl sites of an *ordered layer* form a supercell with hexagonal symmetry, with a lattice constant a' = 6.2 Å (Figure 1c). This inequivalence of the hydroxyl-metal bonding results in a surface corrugation in which the hydroxyl groups bonded to the three-fold Mg_3 sites extend above those bonded to the Mg_2Al sites, as deduced from the covalent radii of the metal atoms (Mg = 1.36 Å, Al = 1.18 Å).

[Figure 1]

Atomic force microscopy (AFM) of the (0001) face of HT (Figure 2) supports ordering of the metal atoms in the HT metal hydroxide layers. High resolution AFM images acquired in aqueous solution reveal a hexagonal periodicity of contrast on the surface with a 6.4 ± 0.3 Å spacing, in near agreement with a' = 6.2 Å for the ordered supercell. Based upon the M-OH bond lengths, the bright regions in the images, which represent features closer to the AFM tip, are assigned to the Mg_3 hydroxyl groups. The irregularity of the observed surface features may be influenced by surface-bound water molecules, surface-bound carbonate anions, and the geometry of the AFM cantilever tip. Indeed, a double-atom tip has been suggested in a theoretical study to be responsible for asymmetric AFM features.[17] Non-ideal tip geometry may also play a role in the irregular features observed in AFM images of montmorillonite and illite clays acquired in ambient air.[18,19] Nevertheless, the AFM data clearly reveal a periodicity of contrast that is consistent with the presence of an ordered supercell in the cationic surface layer. Although ordering of the metal atoms in the hydroxide layers of HT has not been established unequivocally by x-ray analysis, it has been suggested for the related clays $LiAl_2(OH)_7{\cdot}2H_2O$[20] and $LiAl_2(OH)_6{}^+X^-{\cdot}nH_2O$,[21] and for synthetic HT-like phases.[22] This ordered arrangement is most likely a consequence of coulombic interactions within the metal layer, as the average Al^{3+}-Al^{3+} distance is maximized in this configuration.[23]

[Figure 2]

The cationic metal hydroxide layers in HT exhibit two units of positive charge for every 8 metal atoms (i.e., $Mg_6Al_2(OH)_{16}{}^{2+}$), with the charge on the layers compensated by the interstitial anions. The HT sheet exposed at the outer crystal surface therefore possesses one unit of *excess* positive charge for every eight metal atoms because of incomplete charge compensation by the interstitial $CO_3{}^{2-}$ ions. This excess surface charge must be compensated by anionic species adsorbed on the positively charged surface layers. It is reasonable to suggest that exchange between surface-bound ions and more strongly binding anions present in the medium in contact with the surface layer will behave in a manner that mimics ion exchange processes involving the interstitial anions.[13,14] In order to examine this process and the ordering of anionic molecules with respect to the HT layer, we studied the adsorption of the anions of 5-

benzoyl-4-hydroxy-2-methoxy-benzenesulfonic acid (MBSA) on the surface of HT. This compound is of technological interest because of its utility in cosmetics, pesticides, lithographic coating, and ultraviolet screening agents.[24] Notably, MBSA has two acidic hydrogens with relatively low pK_a values (pK_{a1} = 1-2, pK_{a2} = 8),[25] enabling examination of the role of ionicity in the adsorption of the anionic species on the $Mg_6Al_2(OH)_{16}^{1+}$ surface layers.

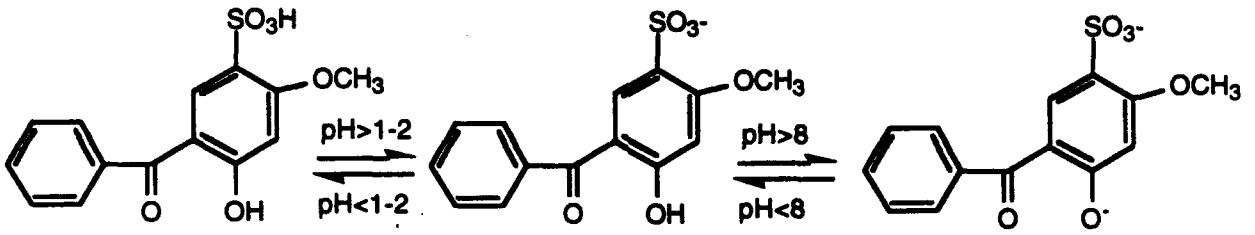

MBSA $MBSA^{1-}$ $MBSA^{2-}$

In aqueous solution under conditions where pH > pK_{a1} or pK_{a2}, adsorption of MBSA will occur on the HT crystal surface to displace weakly bound ions and neutralize the excess charge residing on that surface. Molecular models indicate that the three fold symmetry and size of the sulfonate group on MBSA is ideally suited for hydrogen bonding interactions with the trigonal HT hydroxyl group arrays, which provide three hydrogen-bonding interactions per adsorbed molecule of MBSA (Figure 3).[26] Indeed, weak hydrogen bonding between the hydroxide layers and the interstitial water molecules and anions is commonly accepted.[13a,20b] Close proximity of the negatively charged sulfonate group to the positively charged HT surface layer would also tend to maximize coulombic attractive interactions. Hydrogen bonding and coulombic effects therefore would conspire to favor this orientation over others in which only van der Waals interactions between MBSA and HT are involved.

[Figure 3]

High resolution AFM images of HT in the presence of 1.6 mM MBSA differ substantially from those observed in the absence of MBSA (Figure 4a). In aqueous media at pH = 10.5, $MBSA^{2-}$ is the

predominant species in solution. Under these conditions the hexagonal motif of bare HT transforms into a periodic row structure. The periodicity of contrast conforms to a lattice with constants of 9.6 ± 0.4 Å and 18.2 ± 0.4 Å, based upon average values determined from four independent hydrotalcite images. If each major feature is assigned to a $MBSA^{2-}$ anion, the data is consistent with a monolayer coverage of $\Gamma = 1.06 \times 10^{-10}$ mol cm^{-2}. This coverage is equivalent to one MBSA per 18.9 metal atoms, based on the area per metal atom determined from the x-ray crystal structure of HT. A molecular packing motif of $MBSA^{2-}$ molecules adsorbed on the HT surface that is consistent with the coverage deduced from the AFM data, and takes into account sulfonate binding to hydroxyl group triads (either Mg_3 of Mg_2Al sites) while avoiding steric interactions between $MBSA^{2-}$ anions, is depicted in Figure 4b. This ordered monolayer of $MBSA^{2-}$ anions has P1 plane symmetry and one molecule per unit cell, which has lattice constants of 9.3 Å and 18.6 Å, similar to the values deduced from the contrast in the AFM image. This model corresponds to a monolayer coverage of $\Gamma = 1.11 \times 10^{-10}$ mol cm^{-2} and a ratio of 18.0 metal atoms per $MBSA^{2-}$. This ratio is a consequence, as shown in figure 3, of the constraint that the dianion reside on hydroxyl group triads. However, electroneutrality dictates a stoichiometry of one $MBSA^{2-}$ for every two $Mg_6Al_2(OH)_{16}^{1+}$ units on the surface layer, *corresponding to 16 metal atoms* per $MBSA^{2-}$. This suggests that the adlayer in Figure 4 would have a residual charge of 0.25+ per unit cell, requiring further charge compensation, possibly by solution hydroxide ions. Notably, however, a subset of the AFM images displayed a periodicity corresponding to a lattice with dimensions of 9.2 Å and 17.8 Å, which actually does correspond to 16 metal atoms per $MBSA^{2-}$. The observation of differently sized cells may reflect a small difference in energy between the adlayer structure that is dictated by favorable hydrogen bonding to hydroxyl group triads and the adlayer coverage required by electroneutrality.

[Figure 4]

Reducing the solution pH to values between pK_{a1} and pK_{a2} of MBSA produces a solution rich in the $MBSA^{1-}$ anion. In this case, electroneutrality supports a coverage of adsorbed $MBSA^{1-}$ molecules on HT that is double the coverage for $MBSA^{2-}$, thereby providing a more densely packed surface layer of MBSA

molecules. Indeed, high resolution AFM images of HT in a 1.6 mM solution of MBSA at pH = 6.6 (Figure 5a) reveal a zig-zag row structure with two major features contained in an area bounded by a lattice with constants of 8.0 ± 0.2 Å and 19.3 ± 0.2 Å. The area of the lattice contains 16.6 metal atoms, equivalent to 8.3 metal atoms per $MBSA^{1-}$ and a monolayer coverage of $\Gamma = 2.41 \times 10^{-10}$ mol cm^{-2}. A molecular packing motif that is consistent with this AFM data, while constrained by sulfonate binding to three surface hydroxyl groups, is depicted in Figure 5b. This motif also has P1 plane group symmetry, and consists of alternating rows of $MBSA^{1-}$ anions with an ...ABAB.... pattern, similar to the alternating spacing between the rows of contrast observed in the AFM data. The unit cell of this packing model contains two $MBSA^{1-}$ anions and has dimensions of 8.3 Å and 19.4 Å. The model corresponds to a coverage of $\Gamma = 2.36 \times 10^{-10}$ mol cm^{-2}, which is equivalent to 8.5 metal atoms per $MBSA^{1-}$. This compares favorably to the ideal 8:1 ratio required for electroneutrality and the 8.3:1 ratio deduced from the AFM data. This alternating row motif may be a consequence of the competition between electroneutrality, steric interactions between adjacent $MBSA^{1-}$ anions, and the predisposition of the $MBSA^{1-}$ anions toward binding to the hydroxyl group sites. In the model depicted in Figure 5b, steric interactions are evident from the close proximity of methoxy and benzyl groups of neighboring $MBSA^{1-}$ molecules in alternating rows. These contacts would tend to increase the spacing between these rows at the expense of ideal $MBSA^{1-}$ sulfonate binding to the trigonal surface hydroxyl sites. Indeed, close examination of the AFM data suggest some orientational disorder of the molecular features, which may be a consequence of this competition. The bulky nature of the MBSA molecules introduces a steric component that leads to perturbation of the adlayer structure. Notably, an adlayer comprising shapeless point charges can be constructed that satisfies electroneutrality while maintaining surface bonding of the MBSA sulfonate group to the hydroxyl triad sites for both the mono- and dication. However, construction of such an adlayer with $MBSA^{1-}$ molecules is not possible because of steric interactions between adjacent molecules.

[Figure 5]

These studies indicate that atomic force microscopy provides a unique tool for observing the structure of molecular adlayers on well-defined substrates, with molecular and atomic resolution. The coverage and orientation of 5-benzoyl-4-hydroxy-2-methoxybenzenesulfonate anions onto the surface of the anionic clay HT from aqueous solutions is controlled by coulombic interactions between the MBSA anions and the positively charged clay surface, and by hydrogen bonding interactions between the MBSA sulfonate group and hydroxyl group triads exposed at HT surface layer. These observations illustrate the influence of specific substrate structure and chemical functionality on the orientation and ordering of adsorbates. Molecular-level information of adsorbate structures can be instrumental in advancing understanding of ion exchange processes that occur in these materials, as well as heterogeneous nucleation processes that involve the formation of ordered aggregates on substrate surfaces.[27]

Acknowledgements. We thank Yihan Liu and Suzie Yang (University of Minnesota) for assistance in AFM imaging. This work was supported by the University of Minnesota Center for Interfacial Engineering (NSF Engineering Research Centers Program). The University of Minnesota aknowledges support from the Office of Naval Research.

References

[1] J.M. Lehn, *Angew. Chem. Int. Ed. Eng.* **27**, 89-112 (1988).

[2] G. Desiraju, *Crystal Engineering - The Design of Organic Solids* (Elsevier, New York, 1989).

[3] G. Binnig, C.F. Quate, and Ch. Gerber, *Phys. Rev. Lett.*, **56**, 930-933 (1986)

[4] H. Yamada, S. Akamine, and C.F. Quate, *Ultramicroscopy*, **42-44**, 1044-1048 (1992).

[5] *The Merck Index*, 11th Edition, S. Budavari, Ed. (Merck & Co., Inc., Rahway, N.J., 1989), p. 1419.

[6] (a) P.K. Dutta and M.Puri, *J. Phys. Chem.* **93**, 376-381 (1989). (b) H.C.B. Hansen and R.M. Taylor, *Clay Miner.* **26**, 311-327 (1991).

[7] W.T. Reichle, S.Y. Kang, and D.S. Everhardt, *J. Catal.* **101**, 352-359 (1986).

[8] (a) P.C. Schmidt, K. Benke, *Pharm. Acta Helv.* **63**, 188-96 (1988). (b) Z. Kokot, *Pharmazie* **43**, 249-51 (1988). (c) J.L. Fabregas, J. Cucala, *Int. J. Pharm.* **52**, 173-8 (1989).

[9] M. Rameswaran, E.G. Rightor, E.D. Dimotakis, T.J. Pinnaravaia, *Proc. Int. Congr. Catal. 9th*, **2**, 783-90 (1988).

[10] K. Itaya, H-C Chang, and I. Uchida, *Inorg. Chem.* **26**, 624-626 (1987).

[11] (a) T. Ikeda, H. Amoh, and T. Yasunaga, *J. Am. Chem. Soc.* **106**, 5772-5775 (1984). (b) A. Kachalski, *Nature (London)* **228**, 636 (1970). (c) E. T. Degens, J. Matheja, and T. A. Jackson, *Nature (London)* **227**, 492 (1970). (d) A. Yamagishi, *J. Phys. Chem.* **86**, 2472 (1982).

[12] a) R. Allmann, *Acta Cryst.* **B24**, 972-977 (1968). b) W.T. Reichle, *Solid State Ionics*, **22**, 135-141 (1986). (c) S. Miyata, *Clays Clay Min.* **23**, 369-375 (1975).

[13] S. Miyata, *Clays Clay Miner.* **31**, 305 (1983).

[14] D. L. Bish, *Bull. Mineral.* **103**, 170 (1980).

[15] (a) G.W. Brindley and S. Kikkawa, *Amer. Min.* **64**, 836-843 (1979). (b) C. L. Serna, J. L. Rendon, and J. E. Iglesias, *Clays Clay Miner.* **30**, 180-184 (1982).

[16] L. Ingram and H.F.W. Taylor, *Min. Mag.* **26**(280), 465-479 (1967).

[17] S.A.C. Gould, K. Burke, and P.K. Hansma, *Phys. Rev.* **B40**, 5363-5366 (1989).

[18] (a) J. Ganaes, H. Lindgreen, P.L. Hansen, S.A.C. Gould, and P.K. Hansma, *Ultramicroscopy* **42-44**, 1428-1432 (1992).

[19] H. Hartman, G. Sposito, A. Yang, S. Manne, S. A. C. Gould and P. K. Hansma, *Clays Clay Miner.* **38**, 337-342 (1990)

[20] (a) J.P. Thiel, C.K. Chiang, and K.R. Poeppelmeier, *Chem. Mater.* **5**, 297-304 (1993).

[21] C. J. Serna, J. L. Rendon, and J. E. Iglesias, *Clays Clay Miner.* **30**, 180-184 (1982).

[22] (a) M. C. Gastuche, G. Brown, and M. M. Mortland, *Clay Miner.* **7**, 177-192 (1967). (b) G. Brown and M.C. Gastuche, *Clay Min.* 7, 193-201 (1967). (c) I. Pausch, H.H. Lohse, K. Schurmann, and R. Allmann, *Clays Clay Min.* **34**, 507-510 (1986).

[23] G.W. Brindley and S. Kikkawa, *Amer. Min.* **64**, 836-843 (1979).

[24] (a) J.M. Knox, J. Guin, and E.G. Cockerell, *J. Invest. Dermatol.*, **29**, 435-444 (1957). (b) J.M. Knox, A.C. Griffin, and R.E. Hakim, *ibid.* **32**, 51-58 (1960).

[25] The pK_a values listed for MBSA in this report were determined by titration of 1.6 mmol MBSA in aqueous solution with NaOH.

[26] The MBSA structure depicted here was optimized using MOPAC and the CAChE™ molecular modeling program. The optimized structure compares favorably with that determined from single crystal x-ray diffraction of guanidinium 5-benzoyl-4-hydroxy-2-methoxybenzenesulfonate [V.A. Russell and M.D. Ward, to be published]. The orientation of adsorbed MBSA molecules on the surface of hydrotalcite was optimized using a molecular docking procedure and the CAChE™ molecular modeling program.

[27] (a) L. Addadi, Z. Berkovitch-Yellin, I. Weissbach, I. van Mil, L.J.W. Shimon, M. Lahav, and L. Leiserowitz, *Angew. Chem.* **23**, 346 (1985). (b) E. M. Landau, M. Levanon, L. Leiserowitz, M. Lahav, and J. Sagiv, *Nature*, **318**, 353-356 (1985). (c) E. M. Landau, S. Grayer-Wolf, J. Sagiv, M. Deutsch, K. Kajer, J. Als-Nielson, L. Leiserowitz, and M. Lahav, *Pure. Appl. Chem.*, **61**, 673-689 (1989). (d) P. W. Carter and M. D. Ward, *J. Amer. Chem. Soc.*, **115**, 11521-11535 (1993).

Figure Captions

Figure 1: (a) Hexagonal HT crystals adhered to a freshly cleaved mica substrate by spreading from a water suspension, photographed with an optical microscope. The (0001) plane is parallel to the mica substrate. Hexagonal plate crystals of Mg/Al HT with plate diameters of between 10 and 20 μm and aspect ratios of about 40 were prepared from a dilute aqueous solution containing 0.625 mmol aliminium nitrate nonhydrate, 1.875 mmol magnesium nitrate hexahydrate and 31.25 mmol urea, which was heated in a sealed bottle at 75 °C for one month. The urea slowly hydrolyses to provide both the basicity and carbonate ions necessary for formation of the HT structure. The solid product was filtered, washed with warm water, and freeze dried before characterization and use. X-ray powder diffraction showed the product to be a highly crystalline HT with a basal spacing of 7.6 Å. Chemical and thermal analysis results were consistent with the chemical composition $Mg_6Al_2(OH)_{16}CO_3{\bullet}4H_20$. (b), (c) Structure of HT [$Mg_6Al_2(OH)_{16}CO_3{\bullet}4H_2O$] as viewed normal to ($\bar{1}010$) and (0001) planes. The ($\bar{1}010$) view in (b) illustrates the layered clay structure of HT, which consists of densely packed cationic $Mg_6Al_2(OH)_{16}^{2+}$ sheets separated by interstitial $CO_3^{2-}{\bullet}4H_2O$ layers (the $CO_3^{2-}{\bullet}4H_2O$ units within the anion layers are represented in the image by an oxygen atoms). The cationic sheets exhibit hexagonal symmetry with respect to both the metal and hydroxyl atom positions. In the ordered supercell depicted here, the hydroxyl groups are bonded to either Mg_3 or Mg_2Al sites. The hexagonal supercell, with a' = 6.2 Å, is indicated in (c).

Figure 2: Atomic force microscope (AFM) images of the (0001) face of a HT crystal in aqueous solution: (a) pH = 10.5; (b) pH = 6.6. The pH was adjusted by addition of NaOH to 18 MΩ deionized water. The AFM data reveal a contrast periodicity with hexagonal symmetry that can be described by a lattice constant of 6.4 ± 0.3 Å (the unit cell is overlaid on the AFM data). This value is nearly equivalent to the lattice constant of the ordered HT layer supercell (a' = 6.2 Å). The atomic force microscope (AFM) experiments were performed with a Digital Instruments Nanoscope III scanning probe microscope equipped with Nanoprobe™ cantilevers (Si_3N_4 integral tips with spring constants of 0.3 and 0.06 nm^{-1}, PARK Scientific). Images were obtained in the constant force mode with filters off, an integral gain of 3.0, a proportional gain of 7.0, and a look-ahead gain of 0.0. The "d" scan head was used, which has maximum scan range of 12 x 12 x 4.4 μm^3. The tip scan rate during image acquisition ranged from 25 to 60 Hz, while the applied tip-sample force was maintained at $F_{tip} \leq 10$ nN in solution. AFM experiments

were performed in aqueous solutions with a fluid cell (Digital Instruments), comprising a quartz body with ports for fluid entry and exit. Large single crystals of HT, of approximately 10-20 μm in diameter, were allowed to adsorb from a water suspension onto a freshly cleaved mica substrate. The samples were then removed from the suspension, dried at 120° C for one hour, and attached the mica substrate to a magnetic stainless steel AFM sample disk. The AFM tip was positioned above single HT crystals using an optical microscope prior to imaging. The AFM images have been low pass filtered.

Figure 3: Molecular model of the proposed orientation of $MBSA^{1-}$ or $MBSA^{2-}$ on the surface of HT as viewed (a) normal and (b) 30° off-parallel to (0001) plane of HT. The putative hydrogen bonding interaction between sulfonate oxygens and the hydroxyl triad sites is depicted. This orientation provides three favorable hydrogen bonding interactions between the MBSA ion and the HT surface, and allows for maximum coulombic interactions between the negatively charged sulfonate group and the positively charged HT metal layer.

Figure 4: (a) AFM image of the hexagonal (0001) face of HT in an aqueous solution containing $MBSA^{2-}$ (pH = 10.5). (b) Proposed structure of a molecular $MBSA^{2-}$ layer adsorbed on HT. This packing motif has P1 plane symmetry. The correspondence between the AFM data and the model is revealed by comparison of the unit cells shown, the lattice constants determined from the AFM data (9.6 Å x 18.2 Å) agreeing favorably with those of the model (9.3 Å and 18.6 Å). The sulfonate groups of the $MBSA^{2-}$ anions are assumed to be hydrogen bonded to hydroxyl triad sites as described in Figure 3. The AFM images have been low pass filtered.

Figure 5: (a) AFM image of the hexagonal (0001) face of HT in an aqueous solution containing $MBSA^{1-}$ (pH = 6.6). (b) Proposed structure of a molecular $MBSA^{1-}$ layer adsorbed on HT. This packing motif has P1 plane symmetry. The correspondence between the AFM data and the model is revealed by comparison of the unit cells shown, the lattice constants determined from the AFM data (8.0 Å x 19.3 Å) agreeing favorably with those of the model (8.3 Å x 19.4 Å). The sulfonate groups of the $MBSA^{2-}$ anions are assumed to be hydrogen bonded to hydroxyl triad sites as described in Figure 3. The AFM images have been low pass filtered.

a

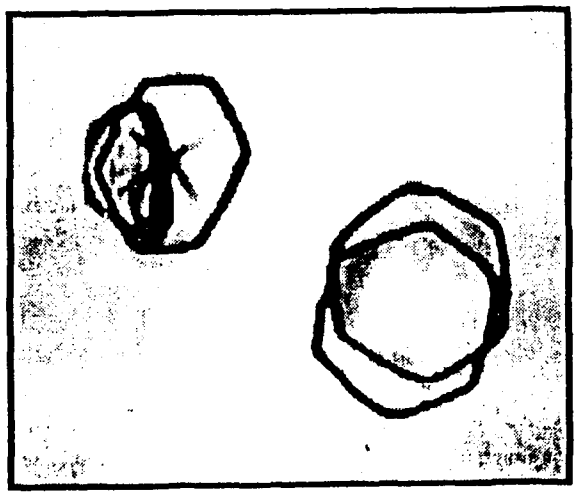

10 μm

b

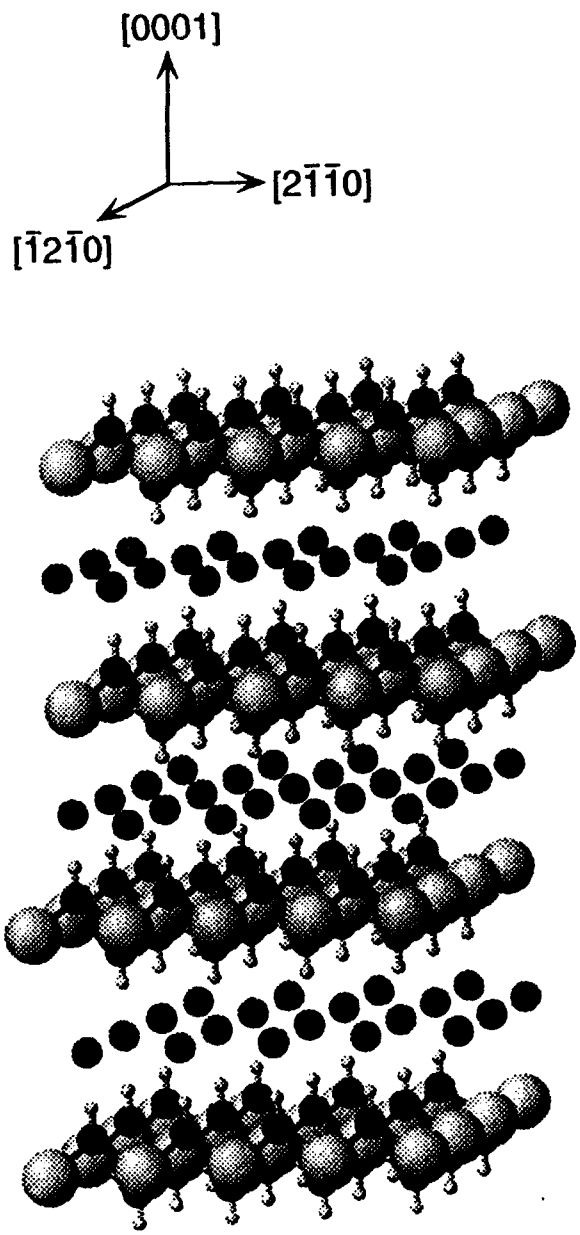
[0001]
[2$\bar{1}\bar{1}$0]
[$\bar{1}$2$\bar{1}$0]

c

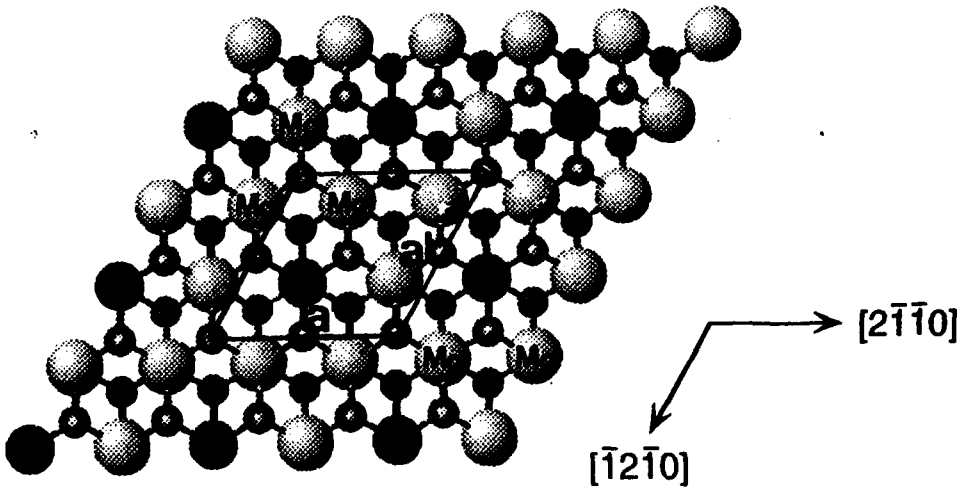
M
M
M
a
a
M
M
[2$\bar{1}\bar{1}$0]
[$\bar{1}$2$\bar{1}$0]

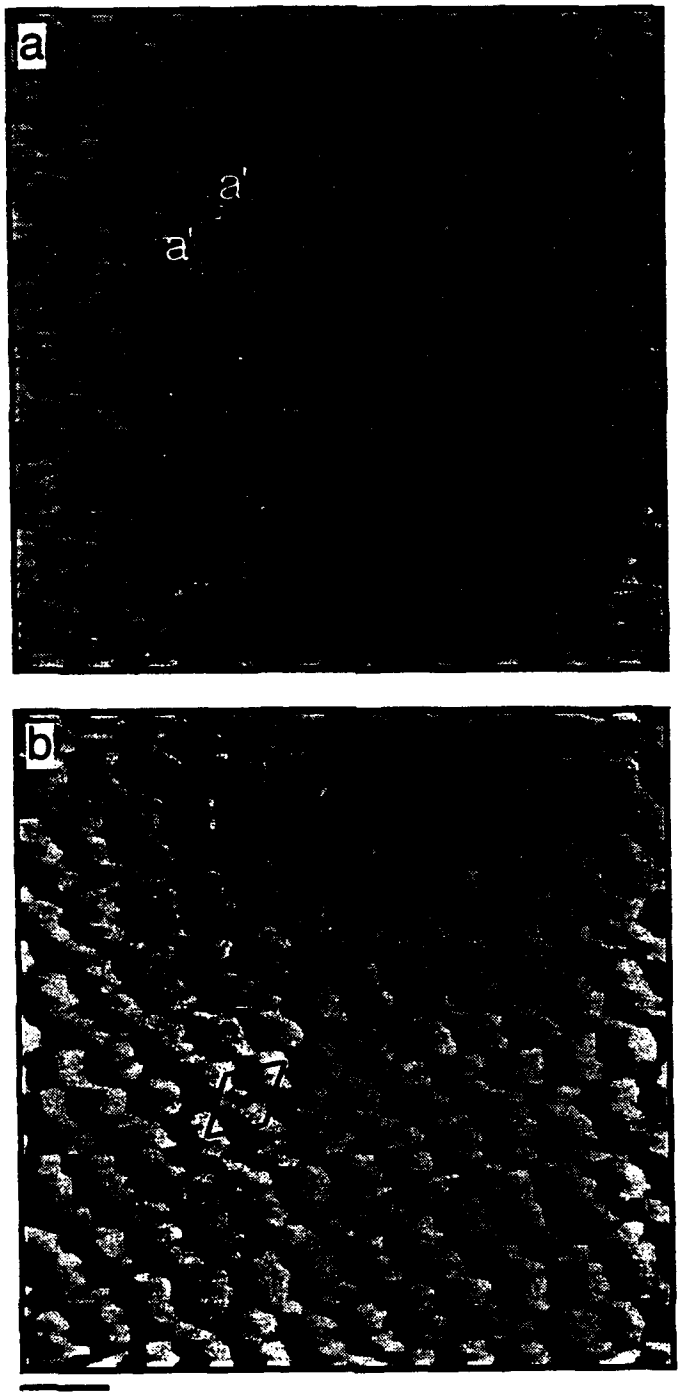
a
a'
a'
b
1 nm

a

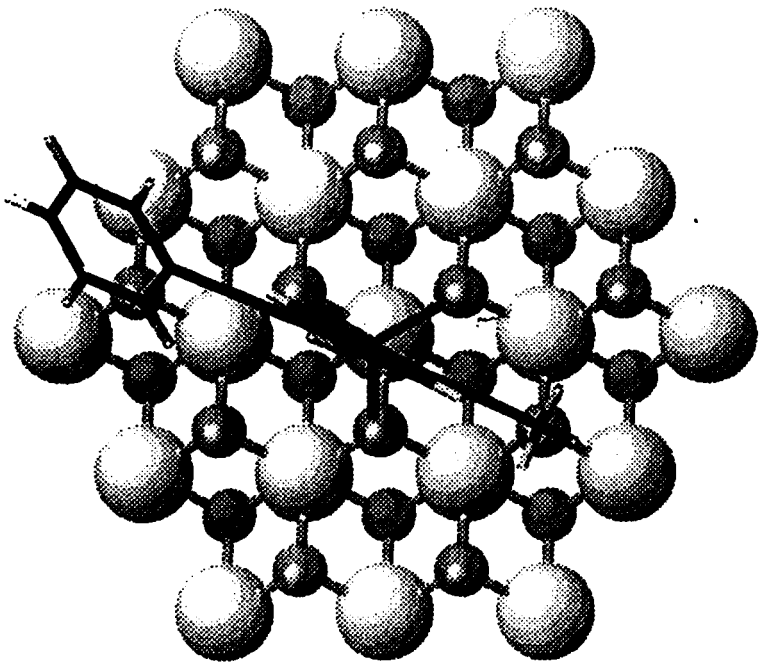

b

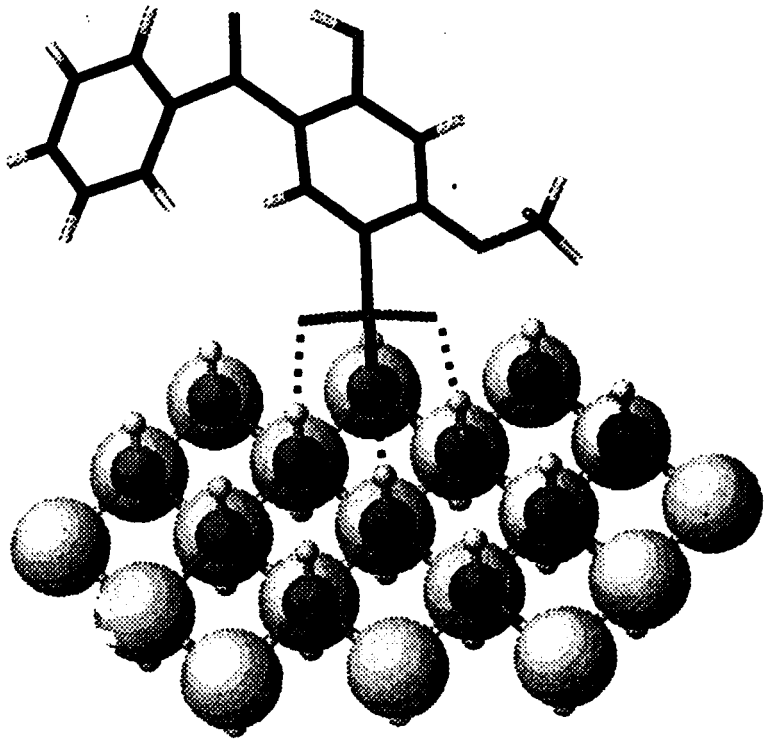

a

1 nm

b

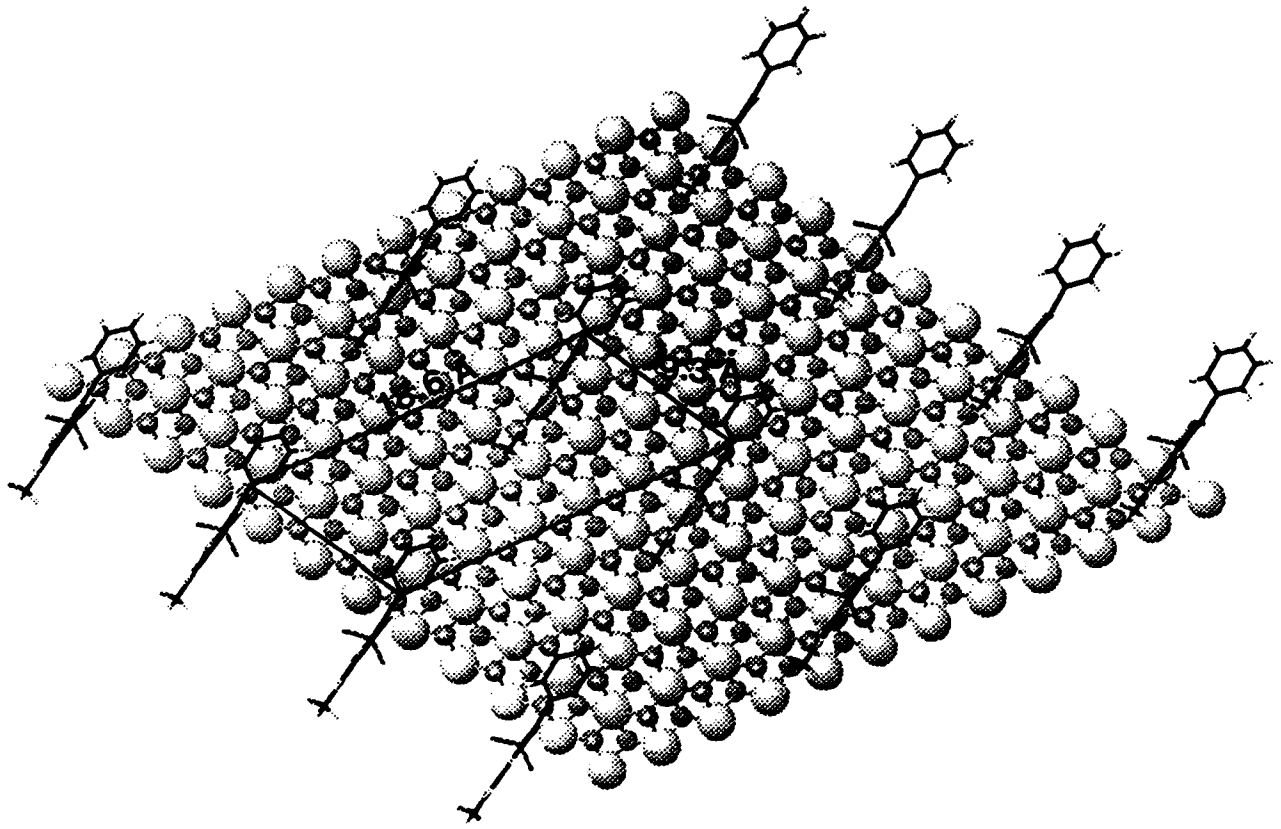

a

b